SUPPORTING INFORMATION

Experimental and theoretical investigation of structures, stoichiometric diversity and bench stability of cocrystals with a volatile halogen bond donor

Katarina Lisac, Vinko Nemec, Filip Topić, Mihails Arhangelskis, Poppy Hindle, Ricky Tran, Igor Huskić, Andrew J. Morris, Tomislav Friščić and Dominik Cinčić**

Table of Contents

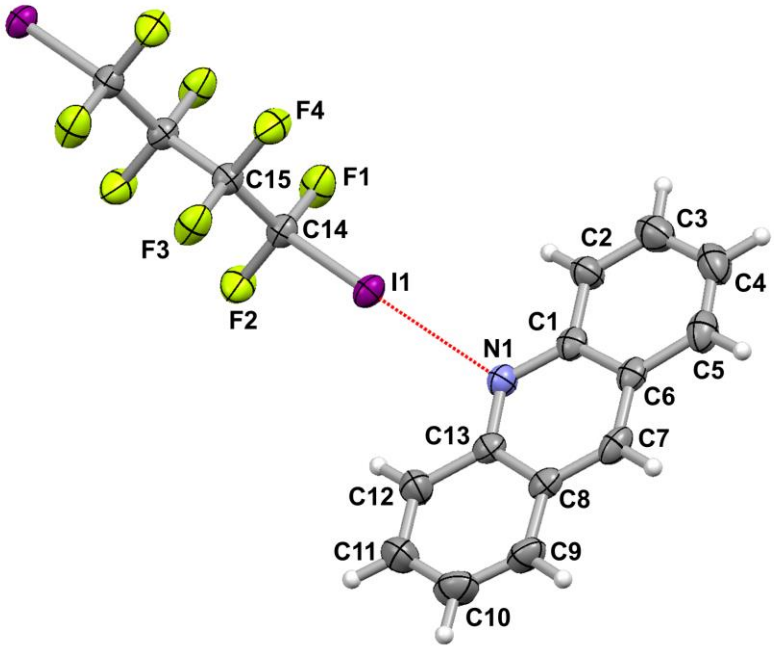

Figure S1. Molecular structure of (**acr**)$_2$(**ofib**) showing the atom-labelling scheme. Displacement ellipsoids are drawn at the 50 % probability level, halogen bonds are marked with red dashed lines, and H atoms are shown as small spheres of arbitrary radius.

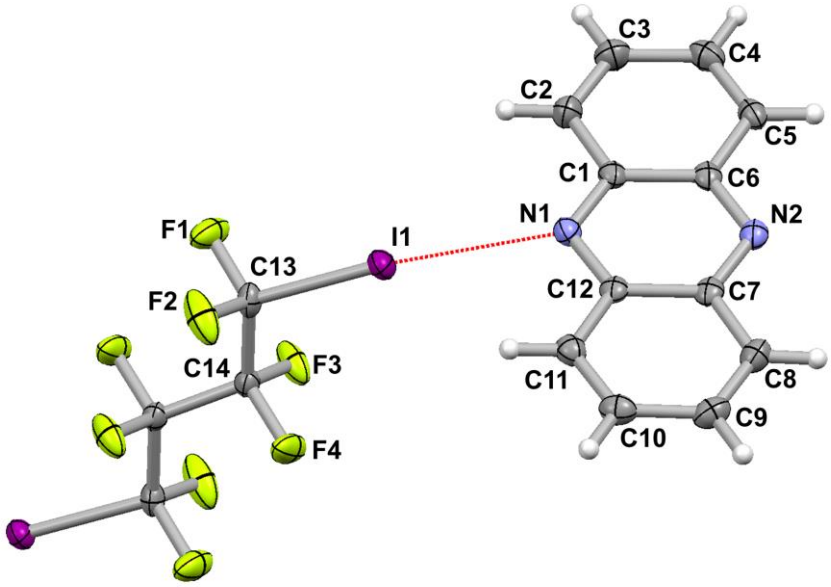

Figure S2. Molecular structure of (**phen**)$_2$(**ofib**) showing the atom-labelling scheme. Displacement ellipsoids are drawn at the 30 % probability level, halogen bonds are marked with red dashed lines, and H atoms are shown as small spheres of arbitrary radius.

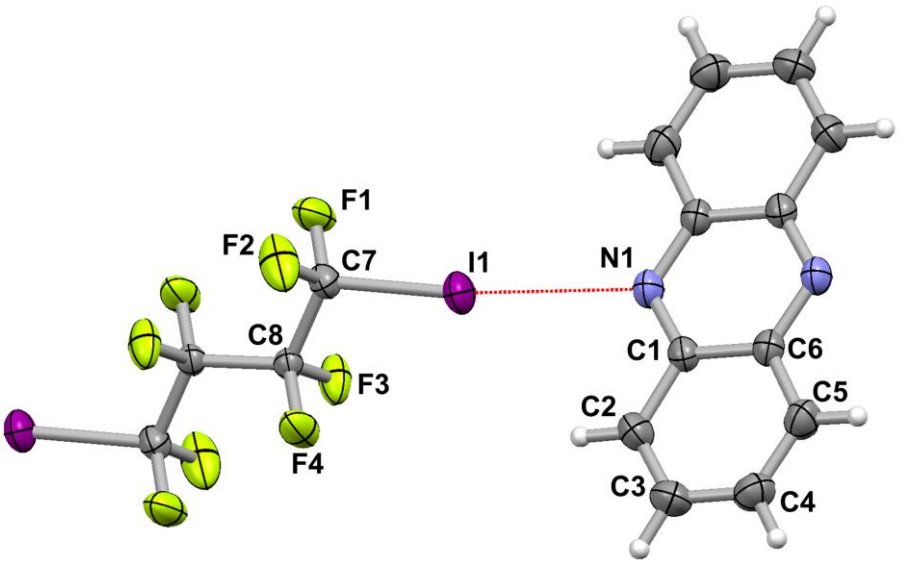

Figure S3. Molecular structure of (**phen**)(**ofib**) showing the atom-labelling scheme. Displacement ellipsoids are drawn at the 50 % probability level, halogen bonds are marked with red dashed lines, and H atoms are shown as small spheres of arbitrary radius.

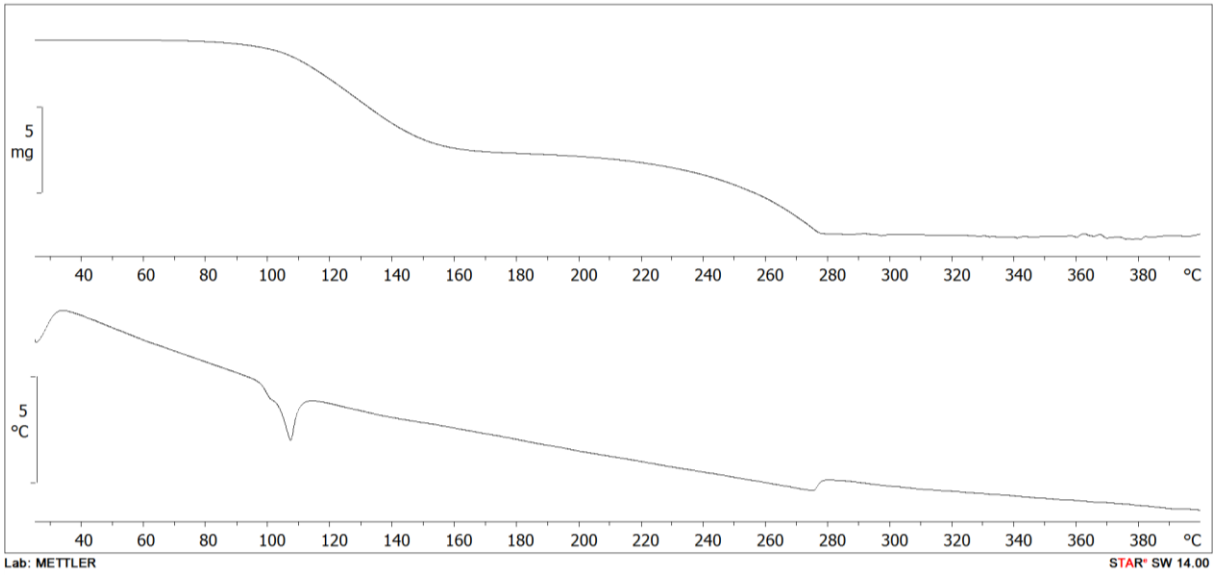

Figure S4. TGA (top) and DTA (bottom) curves for the cocrystal (**acr**)$_2$(**ofib**).

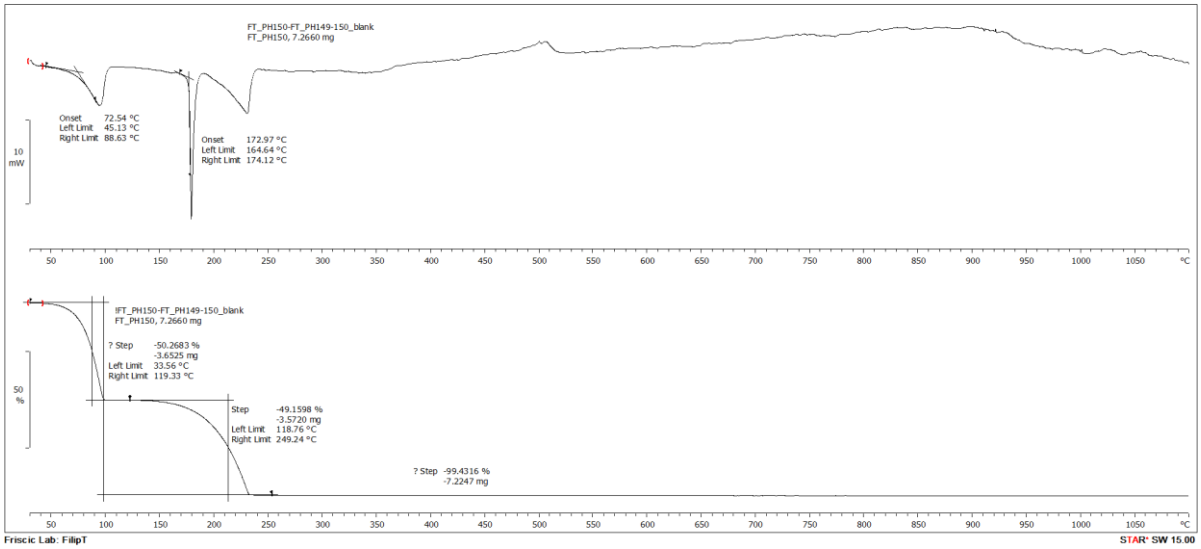

Figure S5. DSC (top) and TGA (bottom) curves for the cocrystal (**phen**)$_2$(**ofib**).

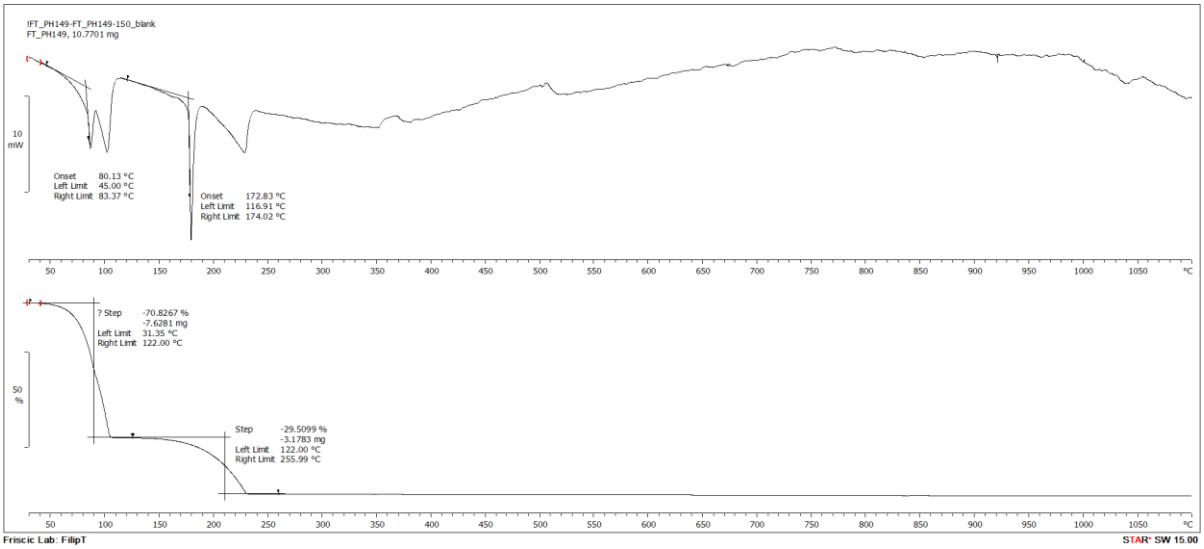

Figure S6. DSC (top) and TGA (bottom) curves for the cocrystal (**phen**)(**ofib**).

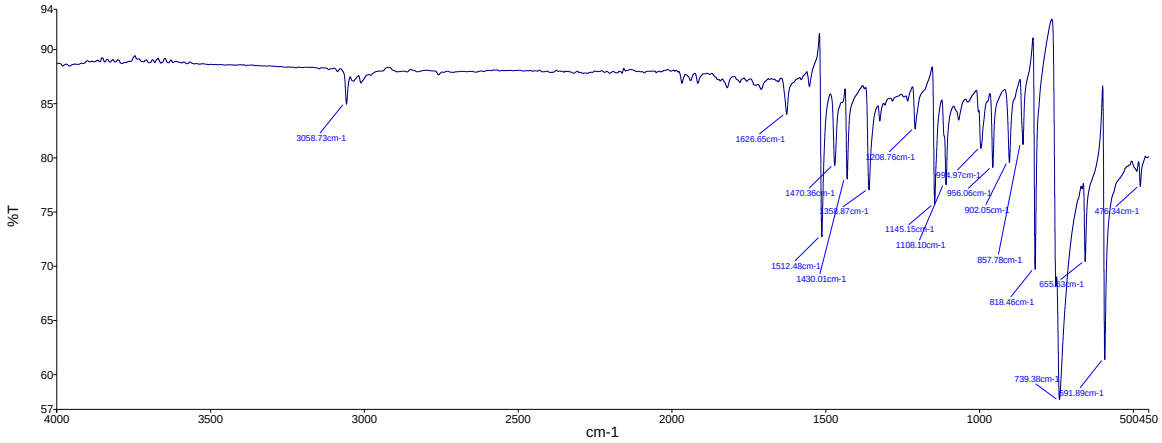

Figure S7. IR-ATR spectrum of solid **phen** reactant.

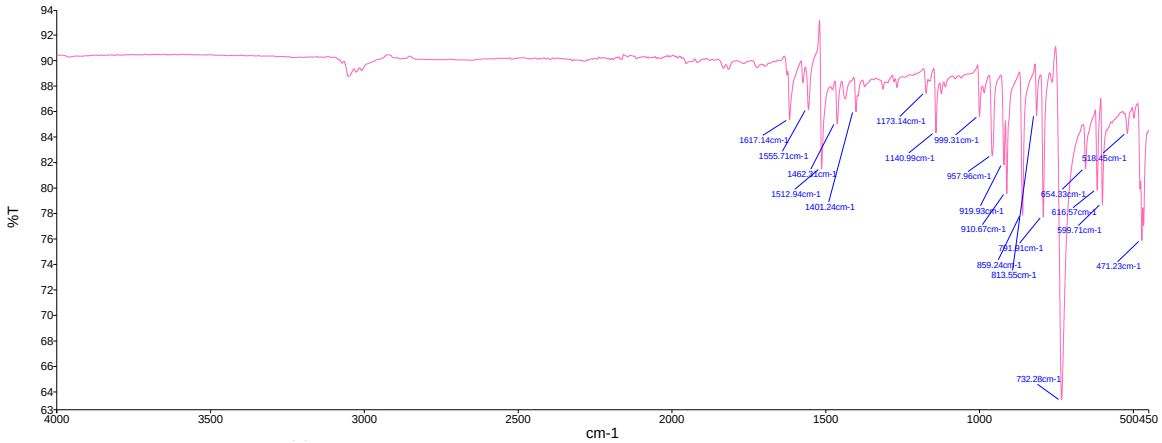

Figure S8. IR-ATR spectrum of solid **acr** reactant.

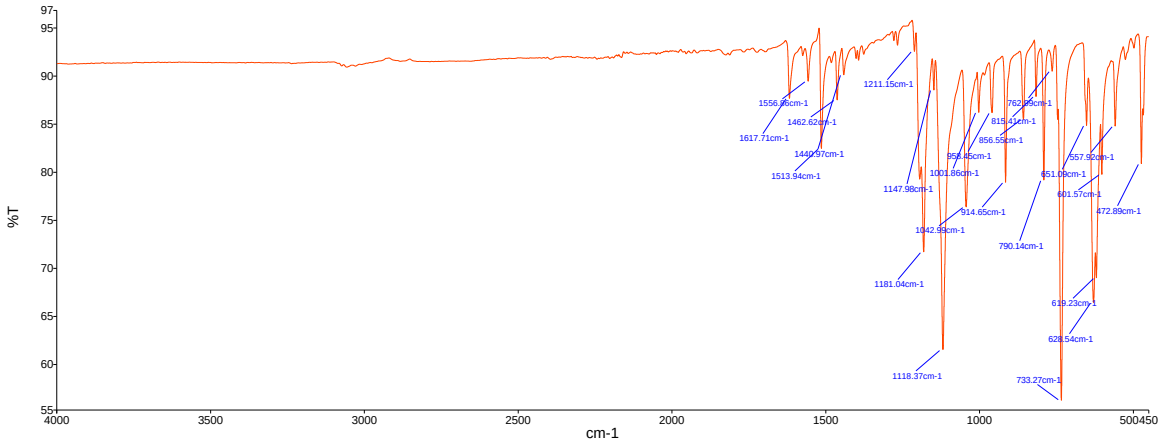

Figure S9. IR-ATR spectrum of the cocrystal (**acr**)$_2$(**ofib**).

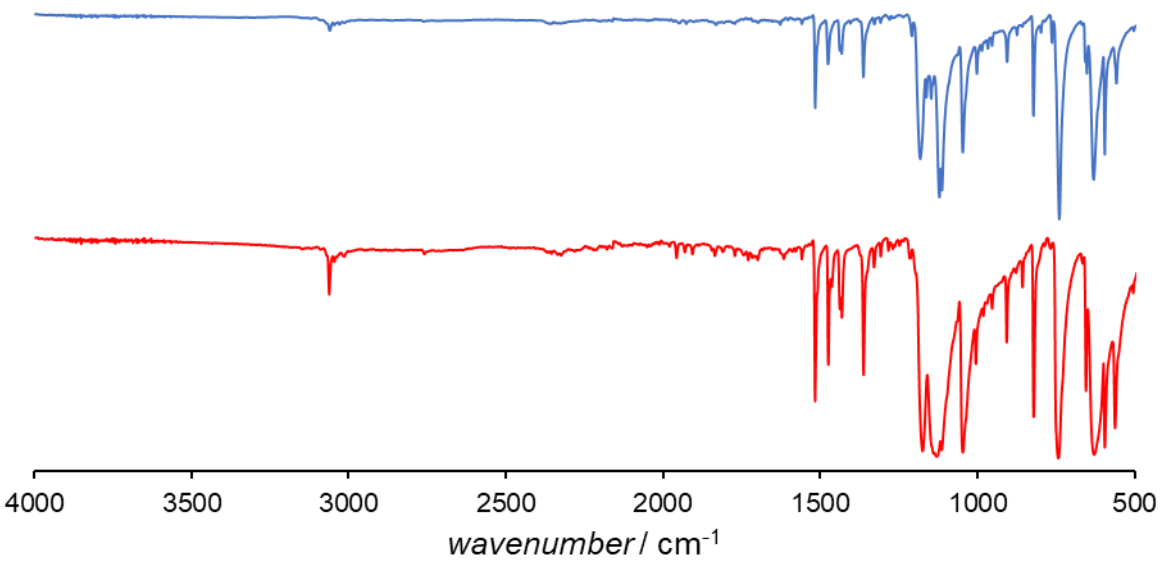

Figure S10. Overlay of IR-ATR spectra of the cocrystals (**phen**)$_2$(**ofib**) (blue) and (**phen**)(**ofib**) (red).